

DOI: 10.17725/rensit.2023.15.223

Specific of microwave radiometers operation on the external distortions conditions

Igor A. Sidorov, Alexander G. Gudkov, Sergey V. Chizhikov, Vitaly Yu. Leushin

Bauman Moscow State Technical University, <https://bmstu.ru/>

Moscow 105005, Russian Federation

E-mail: igorasidorov@yandex.ru, profgudkov@gmail.com, cbigikov95@mail.ru, ra3bu@yandex.ru

Received May 27, 2023, peer-reviewed June 5, 2023, accepted June 13, 2023

Abstract: The influence of external disturbances on the sensitivity and dynamic range of the microwave radiothermograph is considered. The results of an experimental study of the interference situation in the range up to 3 GHz are presented. The diagram of the spectral density of interference adjacent to radio astronomy windows is analyzed. The features of real observed disturbances are investigated. The classification of possible disturbances according to their characteristics is given. Algorithms for discrimination of various types of interference are considered. The sensitivity and dynamic range of the microwave radiometer are evaluated using the pulse noise suppression algorithm.

Keywords: microwave radiothermography, pulse interference, narrowband interference, radiometer sensitivity, dynamic range

UDC 612.087

Acknowledgments: The study was carried out with a grant from the Russian Science Foundation (project No. 19-19-00349P).

For citation: Igor A. Sidorov, Alexander G. Gudkov, Sergey V. Chizhikov, Vitaly Yu. Leushin. Specific of microwave radiometers operation on the external distortions conditions. *RENSIT: Radioelectronics. Nanosystems. Information Technologies*, 2023, 15(3):223-234e. DOI: 10.17725/rensit.2023.15.223.

Contents

1. Introduction (223)
 2. Influence of external interference on the microwave radiometer operation (224)
 3. Algorithm for external impulse noises discrimination (229)
 4. Discussion (232)
 5. Conclusion (233)
- References (233)

1. INTRODUCTION

A microwave radiometer is a highly sensitive receiver of the own radiothermal radiation

from various physical bodies, environments or space objects. Microwave radiometers are mainly used in radio astronomy [1], for remote sensing of the Earth's surface and atmosphere from space [2], from an airplane or unmanned aerial vehicle [3], as well as from various ground carriers [4]. Of particular interest is the use of microwave radiometers in medicine, for non-invasive measurement of the internal temperature of the human body in order to detect malignant neoplasms in the early stages of development, when their therapy is especially effective [5-9]. The probing of the human body by microwave radiometers

simultaneously in several frequency ranges makes it possible to visualize the 3D distribution of the internal thermal field of a person [10]. The input signal of the microwave radiometer is a broadband noise signal - radiothermal radiation, the spectral density of which is described by the well-known Planck formula and Planck's law for blackbody radiation. The distribution of thermal noise amplitudes obeys Gaussian statistics and in the reception band of the microwave radiometer has an almost uniform spectral density, i.e. it represents white noise. For the case of low frequencies, Planck's formula reduces to the Rayleigh-Jeans formula, according to which the intensity of thermal radiation is directly proportional to body temperature. Therefore, the intensity of thermal radiation is usually expressed in units of temperature – degrees on the Kelvin scale. In degrees Kelvin, both the input measured signal of the microwave radiometer and the sensitivity of the radiometer, which is understood as the minimum detectable signal, are expressed.

The sensitivity or minimally detectable signal of an ideal (excluding fluctuations in the gain of a microwave amplifier) full-power radiometer is proportional to the sum of the noise temperatures of the antenna T_A and the first stage of the microwave amplifier T_n and is inversely proportional to the radiometric gain representing the square root of the product of the equivalent width of the input receiving band Δf at the time of accumulation, or integration of the detected signal τ [1].

$$\delta T = \frac{T_a + T_n}{\sqrt{\Delta f \cdot \tau}}. \quad (1)$$

Sensitivity is the most important characteristic of a microwave radiometer along with the dynamic range, which is understood as the ratio of the maximum

undistorted measured signal T_{\max} to the value of the minimum detectable signal δT :

$$D_d = \frac{T_{\max}}{\delta T}. \quad (2)$$

Dynamic range is a dimensionless quantity, which is usually expressed in decibels:

$$D_d [dB] = 10 \lg(D_d). \quad (3)$$

The presence of artificial or natural distortions in the reception band of the microwave radiometer degrades the sensitivity and dynamic range of the radiometer.

The purpose of this article is to evaluate the effect of artificial or natural distortions in the reception band of a microwave radiometer on the sensitivity and dynamic range of the radiometer. And also to evaluate these parameters when using algorithms for discrimination of some special types of distortions, for example, pulse or narrowband distortions.

2. INFLUENCE OF EXTERNAL INTERFERENCE ON THE MICROWAVE RADIOMETER OPERATION

By external distortions, we will understand any signals of natural or artificial origin, other than thermal radiation, falling into the receiving band of the radiometer. Electromagnetic radiation that occurs during spark discharges in the atmosphere – lightning – refers to interference of natural origin. As well as radiation caused by solar flares. Artificial distortions refers to any radiation of artificial origin during arc discharges (electric welding), spark discharges, for example, from candles of a running internal combustion engine, as well as any type of radio transmitters, Bluetooth and Wi-Fi devices and others. Every active

or passive radio user works in the frequency band allocated to him. The distribution of radio airwaves between users is regulated by national legislation, taking into account international agreements. Thus, in the Russian Federation, such distribution is determined by the table approved by the Decree of the Government of the Russian Federation No. 1203-47 dated September 18, 2019 "On Approval of the Table of distribution of Radio Frequency Bands between the Radio Services of the Russian Federation and the Recognition of Certain Resolutions of the Government of the Russian Federation as Invalid". According to the Table, a number of frequency ranges are allocated for the operation of passive means, radiometers and radio telescopes, therefore these ranges are sometimes called "radio astronomy windows". The operation of any active emitters in these ranges is prohibited. But the allocated radio astronomy windows are rather narrow, so frequencies from 1400 to 1427 MHz, that is, only 27 MHz, are allocated in the *L*-band for radio astronomy.

According to the formula (1), the sensitivity of the radiometer is inversely proportional to the square root of the reception bandwidth. Therefore, to increase sensitivity, radio astronomers have only two ways to increase sensitivity:

- 1) reducing receiver noise by reducing the temperature of the microwave amplifier by cooling to the temperature of liquid helium, by using special cryogenic technology, and
- 2) increasing the accumulation time.

For radiometers of remote sensing of the earth from unmanned aerial vehicles, the use of cryogenic technology and an increase in accumulation time are unacceptable. It remains to expand the receiving band, but at the same time, distortions created by active means will inevitably get into the receiving

band of the radiometer. In addition, the dedicated radio astronomy windows are constantly narrowing. So in the *C*-band recently there was a radio astronomy window with a width of more than 200 MHz. According to the latest edition of the "Radio Frequency Band Distribution Table ...", only 10 MHz remained from 200 MHz from 4990 to 5000 MHz. The released frequencies were given for testing of communication facilities according to the 5G standard. So radiometers manufactured before 2019 for the *C*-band now work in distortions conditions.

For medical radiometers – radiothermographs, the situation with external distortions is even worse. Thus, to obtain information about the thermal fields of the human body at a depth of up to 7-10 cm, it is necessary to work in the 700 MHz range with a bandwidth of about 200 MHz. There are no distortions-free bands in this range. The problem is solved with the help of passive anti-distortions devices, either by using special noise-proof antenna applicators, or by conducting analyses in special shielded cameras with a degree of shielding of more than 60 dB. It should be noted that the cost of a shielded camera is almost an order of magnitude higher than the cost of the radiothermograph itself. In addition, there are problems with its placement, assembly and maintenance, which limits the applicability of the method. But even the funds listed are not enough. In addition, the use of shielded cameras is unacceptable both in radio astronomy and in remote radiometric sensing. Therefore, the task of searching for algorithms and methods of operation of radiometers in conditions of external distortions becomes very urgent.

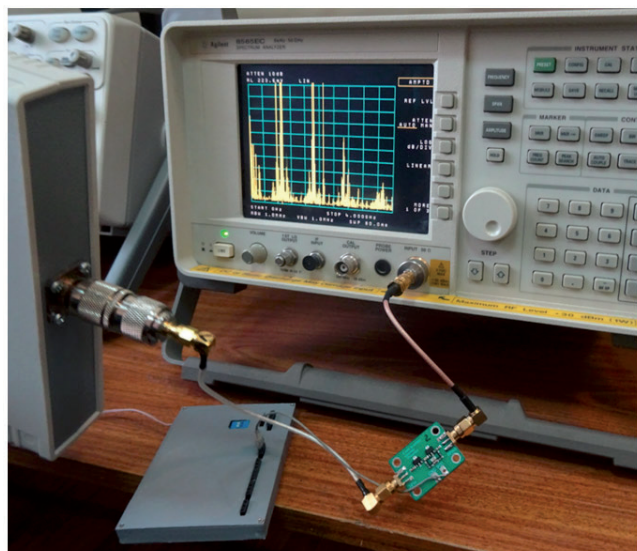


Fig. 1. Distortions spectrum diagram.

To find effective algorithms for the operation of radiometers in distortions conditions, it is necessary to investigate possible types of distortions encountered in practice. To study the frequency distribution of the distortions in the range up to 4 GHz, an experiment was conducted, the scheme of which is shown in **Fig. 1**.

The signal from the broadband antenna was amplified by 40 dB by a low-noise broadband amplifier and fed to the spectrum

analyzer. The distortions spectrogram is shown in **Fig. 2**.

The analysis of the spectrogram shows that the entire ether in the range is quite densely filled with distortions (signals of active means). A small window is observed in the *L*-band and especially strong distortions in the 900 and 1800 MHz bands – interference from GSM cellular networks. Due to the fact that there are practically no free gaps between the distortions, the use of notch filters to filter distortions will be ineffective. The use of known distortions suppression algorithms by digital distortions filtering will also be ineffective.

To study the characteristics of distortions in the time domain, a microwave radiometer with two-references *C*-band modulation was used. The scheme of such a radiometer is known and published [11]. The signal from the output of the power detector was fed to the first channel of the two-channel oscilloscope, a modulation control signal was fed to the second channel, from which the oscilloscope was synchronized. The antenna of the radiometer was either directed into the sky to check for the presence and recording of distortions, or was covered with an absorbing material to register the noise track in the absence of distortions.

At the same time, the output signal of the radiometer was recorded after the synchronous filter and the synchronous detector at an accumulation time of one second.

The view of the noise track (the waveform of the noise signal at the output of the quadratic detector) in the absence of external interference is shown in **Fig. 3**. The modulation control signal is shown against the background of the noise track. The noise signal represents a normally distributed random process. The distribution function

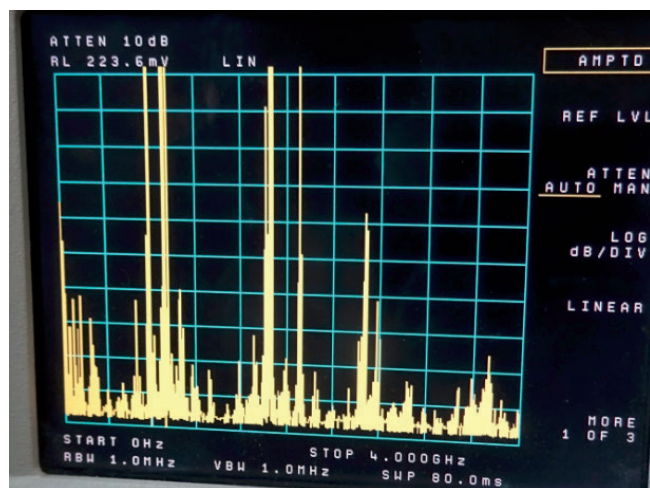


Fig. 2. Distortions spectrogram diagram in the range from 0 to 4 GHz.

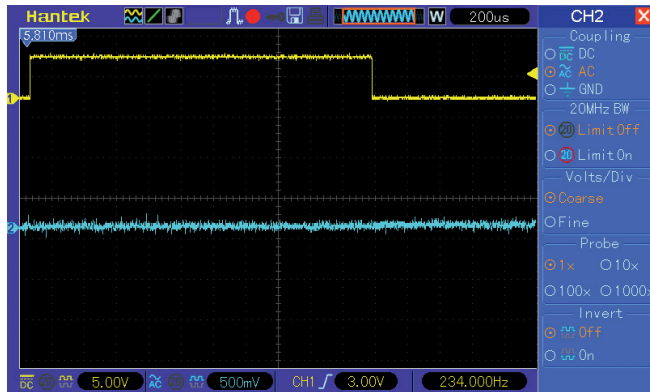


Fig. 3. Noise track view in the absence of external distortions.

of a random process is described by the Gauss formula (4).

$$f(U) = \frac{1}{\sqrt{2\pi\sigma^2}} e^{-\frac{(U-U_m)^2}{4\sigma^2}}, \quad (4)$$

U_{mn} – the average value of the signal or mathematical expectation, σ is the standard deviation or variance.

The signal realization function U , shown in Fig. 3, represents the voltage dependence on time. The voltage is measured in units of Volts, but can be converted to degrees on the Kelvin scale, due to the presence in the radiometer circuit of two internal reference loads with different and known temperatures. It is known that 99.7% of the samples of a normally distributed signal fit into the range $\pm 3 \sigma$. The magnitude of the noise track shown in Fig. 3 can be estimated approximately at 200 mV, which corresponds to a noise temperature of approximately 600 K

The view of the corresponding output signal of the radiometer (Fig. 3) is shown in Fig. 4 as a copy of the screen of the digital processing program, obtained after integrating the signal for one second.

Fig. 4 shows graphs of three values. The upper line in red represents a graph of the values of the "hot" reference load, heated by 50 degrees relative to the "cold" load (blue

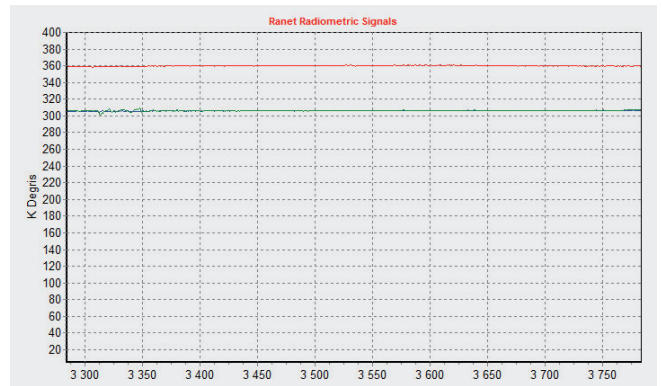


Fig. 4. Radiometer output signal diagram after a second integration.

line), which has a temperature equal to the ambient temperature. The temperature of the "black" body that covered the antenna from distortions is equal to the temperature of the "cold" load (green line). Therefore, their graphs in Fig.4 practically coincide at the level of 305K. At the scale of the graph, the fluctuations of the output signal are not noticeable, since they do not exceed 1 K.

The presence of external distortions significantly changes the picture. Since the power of natural radiothermal signals is extremely small (about – 60 dB), a low-noise microwave amplifier with a large gain is required (about 80 dB with a 50 MHz reception band) so that the amplified noise would significantly exceed the power detector's own noise. With such an amplification, almost any external artificial signal exceeds in magnitude the thermal radiation noise track shown in Fig. 3. An external distortions signal, in the worst case, can overload the amplifier of the first stage when the amplitude of the amplified distortion signal reaches the maximum value of the output signal of the amplifier. In this case, it makes no sense to talk about the sensitivity of the radiometer. It is impossible to work in conditions of such great distortions. But in practice, there are often situations when saturation of the microwave amplifier does not

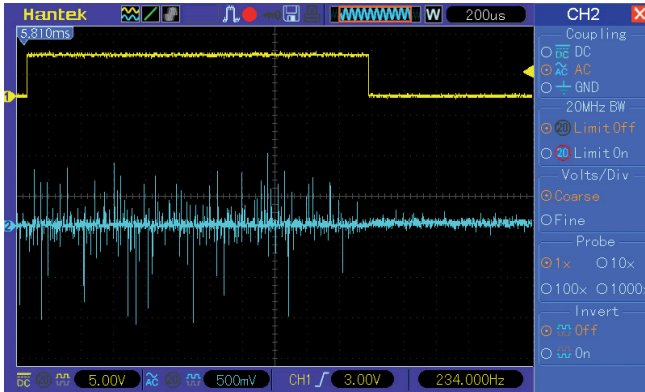


Fig. 5. The power detector output external distortions diagram.

occur, although the distortions exceeds the magnitude of the noise track. An example of a detected signal under such conditions is shown in the oscillogram Fig. 5.

The type of radiometer output signal in the presence of external distortions is shown in Fig. 6.

The range of fluctuations of the output signal in the conditions of external distortions exceeds 300K.

В этом случае минимально обнаружимый сигнал определяется не столько параметрами радиометра, сколько параметрами помехи.

The analysis of the signal shown in Fig. 5 shows that the distortions is not a continuous signal, but a non-periodic sequence of short pulses with different amplitudes. The pulse distortions will be considered short if its

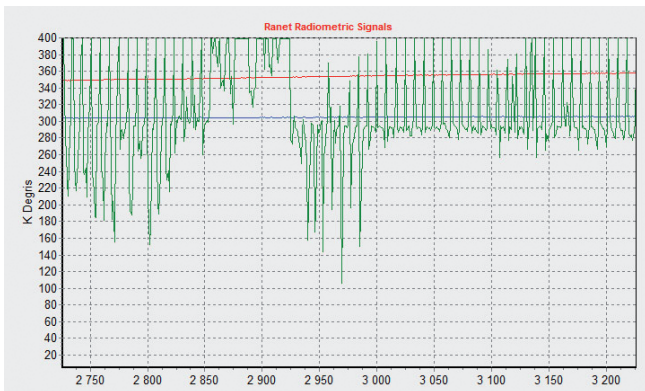


Fig. 6. Radiometer output signal in the conditions of external.

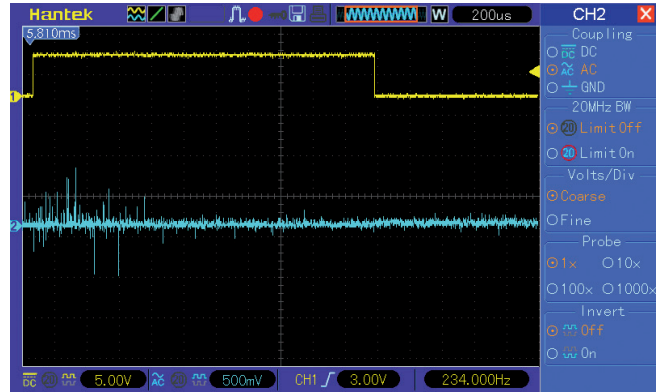


Fig. 7. Example of short pulse interference.

duration is less than the sampling period of the detected signal. In this case, the distortions falls into only one ADC count. This type of distortions is typical for some digital communications and radars for various purposes. If pulse distortions, as in Fig. 5, is received continuously throughout the entire time of signal accumulation, then it is very difficult to take into account their influence and, if possible, eliminate it. Perhaps this is a topic for future research. If the distortions is received only part of the signal accumulation time, then algorithms for detecting, accounting for and suppressing distortions of this type can be proposed. An example of a short pulse distortions is shown in Fig. 7.

It should be noted that in practice there are not only short pulse distortions, but also longer ones, for example, as in Fig. 8. This type of distortions can probably also be

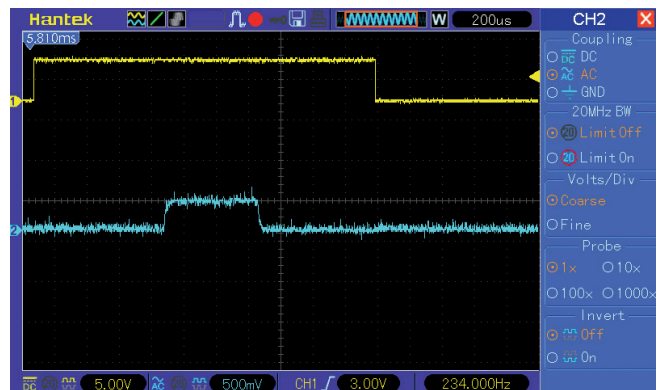


Fig. 8. Example of the long pulse interference.

taken into account and suppressed, but this is the topic of a separate study.

3. ALGORITHM FOR EXTERNAL IMPULSE NOISES DISCRIMINATION

As noted above, the search for effective methods and algorithms for the operation of microwave radiometers in conditions of external distortions is an urgent task. Dissertations and numerous articles are devoted to it solving (for example [12]). But the task is so complex and multifaceted that no common solution has been found so far. The algorithm for taking into account the influence of external distortions for the special case of pulsed non-continuous external distortions is considered below. The algorithm involves detecting the presence of external distortions, filtering out samples containing pulse distortions, further processing the remaining samples to calculate the antenna temperature. It should be noted that in order to apply the algorithm, it is necessary to have registered samples of the signal from the detector output for at least one second. The implementation of the algorithm is possible in two variants: in a pseudo-real time scale and with post-experimental processing of the registered signal.

Post-detector processing of the radiometer signal involves the integration of an analog signal for a sufficiently long time, compared with the modulation period, or the summation of discrete digital samples after converting the analog signal into digital form. When summing N independent samples, the variance of a normal random process decreases by the square root of N times. The actual radiometric gain, represented by the denominator of formula (1), is the square root of the number of

independent signal samples, in accordance with V.A.Kotelnikov's theorem, up to a constant coefficient of 2.

After summing the samples, it is impossible to separate the samples containing distortions from the sum. Therefore, the algorithm must be applied before integrating (summing) the signal. To do this, we need to remember all the samples for the accumulation time. The rate of receipt of samples is determined by the band of the detected signal. It usually does not exceed 50 kHz. Then the sampling frequency will be 100 kHz (in accordance with V.A.Kotelnikov's theorem), and the sampling period is 10 micro seconds. A modulation radiometer with meander modulation receives only half of the time of the modulation period a signal from the antenna, and the second half - signals from internal standards. It is necessary to remember only the samples of the signal from the antenna, since the signals of the standards do not contain external distortions and can accumulate according to a known algorithm. Usually, the isolation between the antenna channel and the reference channels is determined by the quality of the microwave modulator and exceeds 20 dB. If the distortions is so great that it penetrates the channels of the standards, then the microwave amplifier will definitely be overloaded in the antenna channel, and, as noted above, in this case, the distortions suppression algorithms are not effective.

The proposed distortions discrimination algorithm at the first stage involves determining the signal parameters – the average value and dispersion, for a certain short period of time (up to 0.1 of the modulation period) in the absence of distortions. The presence of distortions is determined by the presence of samples, the

value of which deviates from the average value by the amount of tripled dispersion value. If this condition is not met, then other counts are taken for the same period of time. If the desired "reference" interval could not be detected, then the algorithm is not applicable in this situation.

At the second stage, samples are detected throughout the signal accumulation interval, the value of which deviates from the average value by the value of the tripled dispersion and more (the average value and dispersion are determined at the first stage). Further, all detected samples are excluded from the data array.

At the third stage, the summation (averaging) of the remaining samples in the array is performed.

It should be noted that after applying the algorithm, the sensitivity of the radiometer (and, accordingly, the dynamic range) will deteriorate somewhat due to a decrease in the number of independent signal samples summed during the accumulation time. The greater the degradation, the greater the number of samples with distortions (the greater the intensity of the distortions). But this degradation is still less than the deterioration of sensitivity in the presence of distortions and without the use of the algorithm.

The block diagram of the external pulse distortions discrimination algorithm is shown in **Fig. 9**.

In case of inapplicability of this algorithm, two methods are proposed that work in the constant presence of distortions.

The first method is based on iterative distortions suppression. To test the effectiveness of the algorithm, a special program was developed and, based on it, a computer simulation of the distortions

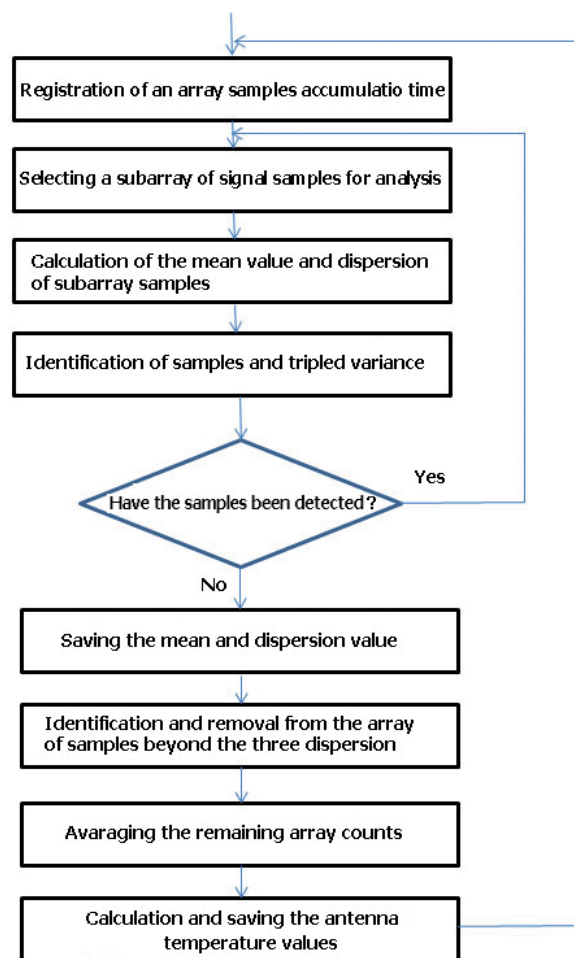


Fig. 9. *The external pulse distortions discrimination algorithm.*

filtering process was carried out. An array of data with parameters close to the parameters of the noise signal at the output of the power detector of the radiometer with a frequency band of about 50 kHz was used as the initial data. The modulation period consists of four intervals of 256 samples. The sampling period is 10 msec. The average value of the simulated signal was taken at the level of 300K, and the variance at the level of 10 degrees. An additional noise process was mixed into the generated data array, simulating a pulse interference with the parameters: the average value (mathematical expectation) at the level of 300K and a variance of 100 degrees. A parameter characterizing the intensity of interference was introduced, numerically equal to the

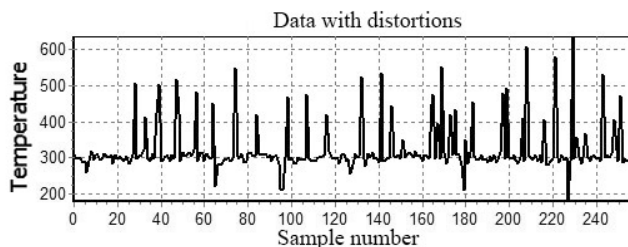


Fig. 10. *Generated data with pulse distortions.*

number of distortions pulses (counts) for one modulation period of 256 counts. The generated data for the distortions parameter of 50 pulses for the modulation period are shown in the graph **Fig. 10**, which are similar to the real recorded data shown in Fig. 7. Different algorithms were used to calculate the mathematical expectation and variance. The iterative algorithm turned out to be the most effective, in which:

1. The mean M and dispersion D are calculated for 256 points.
2. Signal values are revealed a_i , for which $|a_i - M| > kD$ replaced by M .
3. Checking that D has reached the specified value.
4. Skip to step 1 if the value is not reached.

Calculations show that the best result is achieved when $k = 3$.

When noise pulses are added to the original signal, the values of the mathematical expectation and variance of the noise process change. When calculating iterations according to the presented algorithm, after 3-4 iterations, the values of the mathematical expectation and the variance of the noise process return to the set values. A graph of the dependence of the expectation value and the variance of the noise process on the number of iterations is shown in **Fig. 11**.

As can be seen from the graphs, the distortions is almost completely filtered out in five iterations. Of course, the number of

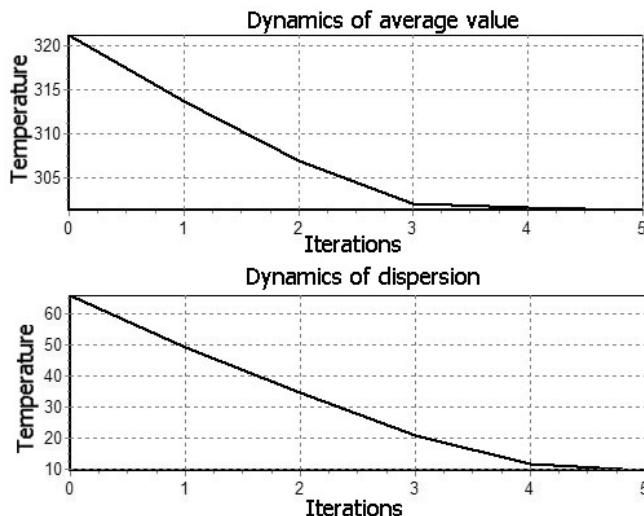


Fig. 11. *The mean value and dispersion changes dynamics.*

iterations required depends on the intensity of the interference.

Another algorithm is based on the analysis of the sample histogram, which leads to the separation of data with distortions and without distortions.

1. A data histogram is being constructed. (**Fig. 12**). As expected, the largest amount of data has accumulated in a cell that corresponds to real data without distortions. It can be seen that 134 values out of 256 have accumulated in this cell.
2. These data are selected, and the average value and variance are calculated.
3. This set is supplemented with those a_i data for which $|a_i - M| < kD$

It follows from **Table 1** that the number of useful signal values has increased to 190. If we take into account that according to

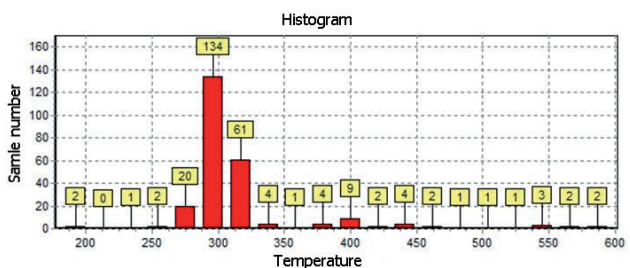


Fig. 12. *Data histogram.*

Table 1

Useful signal			
Iteration	Number	Mean	Dispersion
1	256	318.8793	58.2905
2	134	297.9854	5.7277
3	190	299.5555	8.3838

the parameters of the model, only 50 points were replaced by interference, then we can conclude that these points were removed. They can be replaced by an average value.

The type of signal with filtered interference is shown in **Fig. 13**.

Second sensitivity – the sensitivity of the radiometer with a signal accumulation time of one second, is one of the main parameters of the radiometer that determines the accuracy of measurements and dynamic range. For the signal parameters in the considered model, the second sensitivity, provided there no distortions, would be 0.3 degrees. And in the presence of pulse distortions with the above parameters, the sensitivity would deteriorate by 10 times – up to 3 degrees. Accordingly, the dynamic range will deteriorate by 10 times. When using the proposed interference suppression algorithms, the sensitivity will improve, but will not reach the value obtained for a signal without distortions. The deterioration of sensitivity in this case is not due to an increase in the equivalent noise temperature of the signal, but to a decrease in the number of independent samples of the signal, since part of the samples was removed or replaced by a constant as a result of the application of

algorithms. In this case, the sensitivity after filtering distortions will be 0.37 degrees. The degradation will be 23% and this is significantly better than if the interference was not filtered out. At the same time, the dynamic range will decrease from 43 dB to 42 dB. In the presence of distortions and without the use of distortions suppression algorithms, the dynamic range would be reduced to 33 dB. Of course, the degradation of sensitivity and dynamic range depends on the intensity of distortions.

4. DISCUSSION

The obtained experimental spectrograms and waveforms of a signal with pulse interference, as well as the results of modeling distortions filtering algorithms, allow us to hope for the practical possibility of working in conditions of external pulse distortions. The presented distortions filtering algorithms require testing on real equipment in real conditions. To solve this problem, it is required to digitalize the analog signal from the output of the power detector of the radiometer with a sampling frequency of about 100 kHz and store the data in non-volatile memory. Further processing is carried out in a personal computer using a specialized program. This article discusses distortions received by specialized medical radiothermograph equipment, and it does not consider classical methods of dealing with pulse interference (for example, the median method).

Currently, the conducted research has shown the prospects of these algorithms. However, the use of algorithms requires additional research, including experimental ones, followed by their introduction into data processing programs of the radiothermograph hardware. In case of successful introduction of new devices and

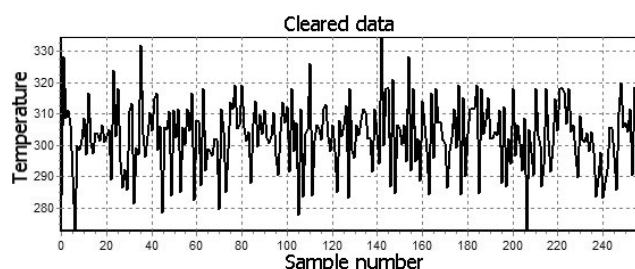


Fig. 13. Data cleared of distortions.

algorithms into the equipment of medical radiothermographs, it will be possible to conduct medical tests and procedures in a regular office without using a special shielded camera, the cost of which significantly exceeds the cost of the radiothermograph itself. Due to the exclusion of the cost of a special shielded camera from the total cost of the necessary equipment, the method of microwave radiothermography using a radiothermograph will become more accessible and widespread.

5. CONCLUSIONS

As a result of experimental studies, calculations and modeling, the following new results were obtained:

- waveforms of real external pulse interference of a microwave radiometer in the C-band were obtained;
- the analysis of the operation of the microwave radiometer in the conditions of pulse distortions was carried out;
- the influence of external pulse distortions on the sensitivity and dynamic range of the microwave radiometer was evaluated;
- the algorithm of detection, accounting and discrimination of pulse distortions is proposed;
- the sensitivity and dynamic range of the microwave radiometer were evaluated, taking into account the suppression of external pulse interference.

REFERENCES

1. Yesepkina NA, Korolkov DV, Pariyskiy YuN. *Radio telescopes and radiometers*. Moscow, Nauka Publ., 1973, 416 p.
2. Kerr YH, Waldteufel P, Wigneron, J-P, Martinuzzi J-M, Font J, Berger M. Soil moisture retrieval from space: The soil moisture and ocean salinity (SMOS) mission.

3. Verba VS, Gulyaev YuV, Shutko AM, Krapivin VF (Eds.). *Microwave Radiometry of Land and Water Surfaces: From Theory to Practice*. Sofia, Marin Drinov Academic Publishing, 2013, 296 p.
4. Sidorov IA, Gudkov AG, Oblivantsov VV, Ermolov PP, Novichikhin EP, Leushin VYu, Agandeev RV. Radiometric remote determination of soil moisture portraits in a vineyard in Crimea. *Electromagnetic waves and electronic systems*, 2022, 27(5):65-70; <https://doi.org/10.18127/j15604128-202205-09>.
5. Evgeny P. Novichikhin, Igor A. Sidorov, Vitaly Yu. Leushin, Svetlana V. Agasieva, Sergey V. Chizhikov. Detection of a local source of heat in the depths of the human body by volumetric radiothermography. *RENSIT: Radioelectronics. Nanosystems. Information Technologies*, 2020, 12(2):305-312. DOI: 10.17725/rensit.2020.12.305.
6. Ahmed M Hassan, Magda El-Shenawee. Review of Electromagnetic Techniques for Breast Cancer Detection. *IEEE Reviews in biomedical engineering*, 2011, 4:103-118. DOI: 10.1109/RBME.2011.2169780.
7. Vesnin S, Turnbull AK, Dixon JM, Goryanin I. Modern Microwave Thermometry for Breast Cancer. *J. Mol. Imaging Dyn.*, 2017, 7(2):136-141. DOI: 10.4172/2155-9937.1000136.
8. Gudkov AG; Leushin VY, Sidorov IA, Vesnin SG, Porokhov IO, Sedankin MK, Agasieva SV, Chizhikov SV, Gorlacheva EN, Lazarenko MI et al. Use of Multichannel Microwave Radiometry for Functional Diagnostics of the Brain. *Biomed. Eng.*, 2019, 53:108-111.
9. Sedankin M, Chupina D, Vesnin S, Nelin I, Skuratov V. Development of a miniature

- microwave radiothermograph for monitoring the internal brain temperature. *East. Eur. J. Enterp. Technol.*, 2018, 3:26-36.
10. Sidorov IA, Gudkov AG, Leushin VY, Gorlacheva EN, Novichikhin EP, Agasieva SV. Measurement and 3D Visualization of the Human Internal Heat Field by Means of Microwave Radiometry. *Sensors*, 2021, 21:4005, doi: 10.3390/s21124005.
11. Sidorov IA, Gudkov AG, Agasieva SV, Khokhlov NF, Chernikov AS, Vagapov Y. A portable microwave radiometer for proximal measurement of soil permittivity. *Computers and Electronics in Agriculture*. 2022, 198(2):107076. DOI: 10.1016/j.compag.2022.107076.
12. Fedoseeva EV, Shchukin GG, Rostokin IN, Rostokina EA. Compensation of interference in the operation of microwave radiometric systems. *Radio engineering and telecommunication systems*, 2014, 1(13):50-62.